

Review

Fiber Laser Sensor Configurations for Refractive Index, Temperature and Strain: A Review

D. Jauregui-Vazquez ^{1,*}, J. A. Alvarez-Chavez ², T. Lozano-Hernandez ³, J. M. Estudillo-Ayala ³,
J. M. Sierra-Hernandez ³ and H. L. Offerhaus ²

- ¹ Centro de Investigación Científica y de Educación Superior de Ensenada (CICESE), División de Física Aplicada-Departamento de Óptica, Carretera Ensenada-Tijuana, No. 3918, Zona Playitas, Ensenada 22860, Mexico
- ² Optical Sciences Group, University of Twente, Drienerlolaan 5, 7522 Enschede, NB, The Netherlands; j.a.alvarezchavez@utwente.nl (J.A.A.-C.); h.l.offerhaus@utwente.nl (H.L.O.)
- ³ Departamento de Ingeniería Electrónica, División de Ingenierías Campus Irapuato Salamanca, Universidad de Guanajuato, Carretera Salamanca-Valle de Santiago, Salamanca 36885, Mexico; t.lozanhernandez@ugto.mx (T.L.-H.); jm.sierrahernandez@ugto.mx (J.M.S.-H.)
- * Correspondence: djauregui@cicese.mx

Abstract: Fiber laser sensors have been present for almost four decades as versatile sensing devices with a simple demodulation process, high sensitivity, and competitive resolution. This work discusses the most representative fiber laser sensor configurations employed for detecting critical parameters such as temperature, refractive index, and strain. However, essential information about other interesting parameters that have been measured is considered in this manuscript. Concurrently, the sensing elements and principle operation are described. Furthermore, these configurations are analyzed in terms of their principle of operation, sensitivity, gain medium, and wavelength operation range. According to the literature reviewed, fiber laser sensors offer the possibility of new interrogation techniques and simultaneous, independent detection. Considering interferometric fiber sensors, the fiber laser sensors offer high brightness, good output power, and high resolution. As a result, it is demonstrated that fiber laser sensors are a robust alternative for multiple sensing applications.

Keywords: fiber optics; fiber lasers; sensors; temperature; refractive index; strain



Citation: Jauregui-Vazquez, D.; Alvarez-Chavez, J.A.; Lozano-Hernandez, T.; Estudillo-Ayala, J.M.; Sierra-Hernandez, J.M.; Offerhaus, H.L. Fiber Laser Sensor Configurations for Refractive Index, Temperature and Strain: A Review. *Photonics* **2023**, *10*, 495. <https://doi.org/10.3390/photonics10050495>

Received: 21 March 2023
Revised: 19 April 2023
Accepted: 23 April 2023
Published: 26 April 2023



Copyright: © 2023 by the authors. Licensee MDPI, Basel, Switzerland. This article is an open access article distributed under the terms and conditions of the Creative Commons Attribution (CC BY) license (<https://creativecommons.org/licenses/by/4.0/>).

1. Introduction

The first laser was reported by T.H. Maiman in 1960 [1], and since then, several sensing technologies based on lasers have been demonstrated. At around the same time, optical fiber sensors were introduced as a versatile technique [2]. Moreover, the first optical amplifier was reported in the same decade [3]. A few decades later, Erbium optical fiber amplifiers opened the possibility of new sensing technologies [4,5]. The next decade, the fiber laser sensor emerged as a sensing alternative based on its tuning capability [6–11]. This feature offers a simple and not intricated demodulation process. This capability is linked to the gain medium and the sensing head characteristics. The wide variety of gain material elements offer different wavelength operations ranging from the visible to the near-infrared; as a result, it is possible to explore different applications. At the same time, each gain medium has challenges such as the performance degradation caused by concentration quenching [12]. Other challenges are related to the fiber laser configuration itself (ring or linear); here, the high losses generated by long fiber sections and spectral broadening are critical aspects to be considered. Despite these challenges, the fiber laser sensors offer advantages such as good signal-to-noise ratio (SNR), narrow linewidth, high sensitivity, practical detection limits, and high resolution. These advantages are added to the fiber optic sensor characteristics: immunity to electromagnetic noise, resistance to aggressive environments, and being lightweight and compact.

The first fiber laser sensors were proposed using fiber Bragg gratings (FBG) [6,7,13]; in these works, special attention was paid to detecting strain and temperature. G. A. Ball et al. proposed a distributed Bragg reflector and a linear fiber laser cavity to monitor temperature [7]; here, it was possible to detect the temperature at three locations. Additionally, S.M. Melle et al. reported a simple linear fiber laser cavity to monitor strain, where the strain was applied over an FBG [13]. At the same time, optical fiber gyroscopes were proposed based on fiber lasers [9]. The Sagnac reflector was introduced into a fiber laser cavity to monitor rotation.

For some decades, FBGs were the predominant sensing element [7,13–19]; however, other fiber laser configurations based on the Brillouin effect were demonstrated for temperature and strain [20–22]. Furthermore, the FBGs started being combined with Fabry-Perot [23], Sagnac [24], and Mach-Zehnder [25] interferometers to improve the fiber laser sensor performance. The fiber laser sensor was also explored for gas concentration detection [14,26]; here, an FBG tunes the laser emission at a specific gas absorption range.

In the last decades, several research groups have employed different optical fiber structures as sensing heads in fiber laser sensors: tapers [27], multimode interference filters [28], and all fiber interferometers [29–32]; these elements improve the possibility of tuning a lasing mode. As a consequence, multiple parameters have been detected using fiber laser sensors: refractive index [33,34], curvature [35,36], strain [37–39], temperature [40–44], magnetic field [45,46], liquid level [27,47], torsion [48], rotation [49], gas concentration [29,50], gas pressure [51,52], relative humidity [32,53], and ultrasound [54]. In many of these works, the sensitivity reported by prior works was improved, and simultaneous detection of multiple parameters was also demonstrated. In this manuscript, we present a comprehensive analysis of the current status of fiber laser sensor technology. The typical configurations and their principle of operation are analyzed. In addition, the sensitivity and sensor performance are compared and discussed based on a specific physical parameter.

2. Fiber Laser Sensor Configurations and the Principle of Operation

This review focuses on fiber laser cavities employed for sensing purposes. As a result, we divide the principle of operation as follows:

- Continuous Wave (CW) Fiber Laser Sensor
- Brillouin Fiber Laser Sensor
- Mode-locked Fiber Laser Sensor
- Distributed Feedback Fiber Laser Sensor

2.1. Continuous Wave (CW) Fiber Laser

The tunable fiber laser operated in CW is the most common fiber laser sensor. This technique can shift a single lasing mode while a physical parameter is applied over the sensing head (SH). Here, two fiber laser cavities can be found: linear and ring.

Both employ the following main elements: an optical pump source, a wavelength division multiplexor (WDM), a segment of optical fiber as the gain medium, a sensing head (SH), a polarization controller (PC), and an optical fiber coupler (OC). These elements are interconnected to form the cavities mentioned above (see Figure 1). For the ring laser configuration, the light from the pumping light source is launched to the fiber laser cavity by the WDM; afterward, the light reaches the doped optical fiber (DOF), the gain medium. In Figure 1a,c, the OC monitors one portion of the light in the fiber laser cavity and provides the signal feedback to ensure the light oscillation into the ring fiber laser cavity; the SH can be used in transmission mode (Figure 1a) or reflection mode (Figure 1c), in the last case it is necessary, and optical fiber circulator (OFC). The optical fiber isolator ensures unidirectional mode operation. In addition, the PC sets the polarization state in the fiber laser cavity; this polarization stage is aligned to the plane of incidence [55]. In the linear fiber laser shown in Figure 1b,d, the isolator and the SH provide a reflection signal to ensure light oscillation. Meanwhile, in Figure 1d, the OC and the isolator guarantee light oscillation. The fiber laser sensors operated in CW employ the tunable effect of a single lasing mode. To achieve a

single lasing mode, it is essential to avoid the spatial hole burning (SHB) effect [56]; here, since the ring laser cavity operates in one direction, it eradicates this effect. Ensuring that a single lasing mode is propagated in a linear laser cavity with a short section of the gain medium is essential. In addition, a wide tunable range is achieved by controlling the gain-losses profile in the fiber laser cavity. In a closed cavity, the gain (G) is linked to the cavity losses (β). The feedback signal sent to the doped fiber can saturate the gain when the losses are minimal. Here, the gain of the doped fiber $G(\lambda)$ made a match with the optical feedback cavity losses $\beta(\lambda)$ for a specific wavelength (λ), therefore, it is possible to obtain $\beta(\lambda) < G_0(\lambda)$ [12,55], where $G_0(\lambda)$ is the unsaturated gain. Considering that the saturated gain medium provides a flat amplified spontaneous emission (ASE) spectrum [55], it is possible to tune the lasing mode over the flat ASE spectrum by controlling the gain-losses profile. To achieve this, the gain of the doped fiber needs to generate a deep saturation state; then, when a small gain alters the losses equilibrium, the lasing output is shifted for the wavelength that guarantees the condition $\beta(\lambda) < G_0(\lambda)$. Once the single mode operation is achieved and it is possible to have a wide tunable range, the sensing principle can be implemented by applying the parameter of interest to the SH; here, the SH governs the gain-losses profile and provides a tunable response related to the parameter applied. As mentioned above, the SH can operate in reflection or transmission mode. For instance, for an SH composed of interferometers, the interference signal's peaks and valleys (reflection or transmission) are shifted by an external perturbation, altering the gain-losses points. When an FBG is employed, a peak component is reflected; however, at the same time, a deep loss point is transmitted. In both cases, the $\beta(\lambda) < G_0(\lambda)$ relation is controlled.

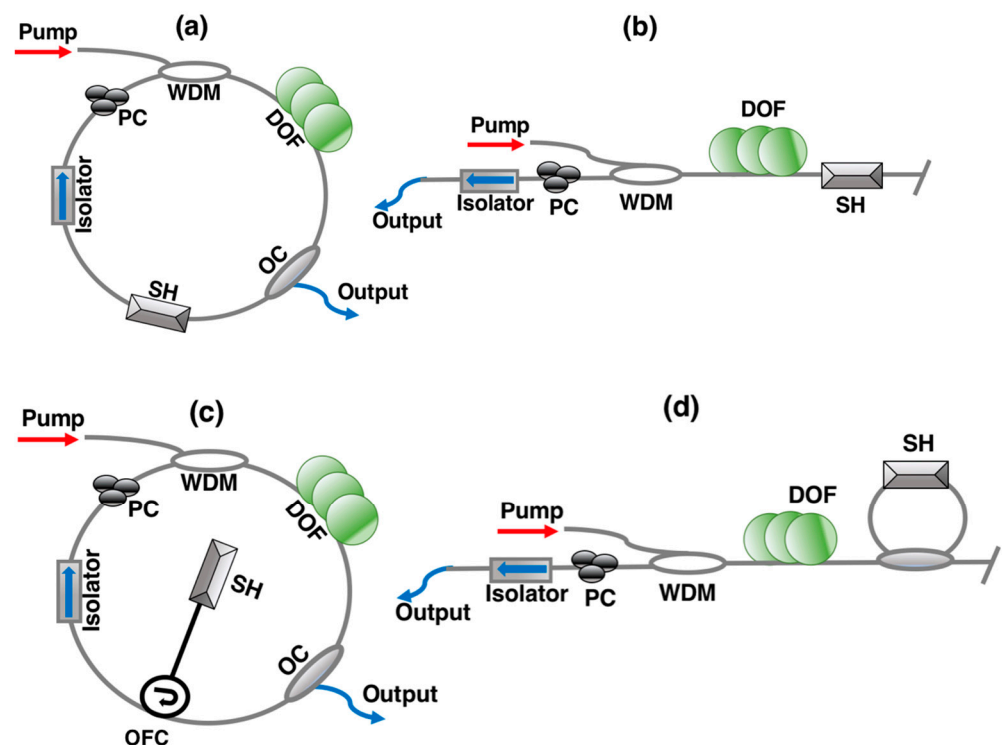


Figure 1. Typical (a) ring, and (b) linear, fiber laser cavities proposed for CW fiber laser sensors. Alternative (c) ring, and (d) linear, configurations using the SH in reflection and bi-directional mode, respectively.

Usually, the interferometers used in the transmission mode are Sagnac and Mach-Zehnder; the transmission signal is more significant than the reflected signal. Meanwhile, the interferometers used by the configurations in reflection mode are Michelson and Fabry-Perot. These interferometers can also be used in a linear fiber laser sensor, and the SH can also be set to reflection mode (Figure 1b) or transmission mode (Figure 1d).

The FBG can be used in all the configurations shown in Figure 1. It is important to mention that by using optical fiber couplers, the sensing SH can be located differently; however, it is critical to determine whether the SH is operated in reflection or transmission mode. Additionally, to the reflection/transmission mode operation difference between the mentioned interferometers, the optical path difference is an important aspect to consider for the fiber laser cavity design. Usually, the interferometers operated in reflection mode exhibit a double phase difference than those operated in the transmission mode; this is related to the optical path. As a result, it is possible to observe a dual-wavelength emission.

As mentioned above, the first fiber laser sensors were based on FBGs. S.M. Melle et al. proposed a linear fiber laser sensor for strain monitoring in 1993 [13]. The strain was applied over an FBG to achieve a tunable effect. This configuration was also explored for temperature detection by G. A. Ball et al. [7]; the tunable effect was also used for this parameter. Here, the authors use a linear fiber laser sensor with multiple FBGs. The following decade, a ring fiber laser sensor was proposed by O. Frazão et al. [17]. In their work, two FBGs were set into the ring cavity for curvature detection; the curvature was estimated as the peak wavelength was shifted. A dual fiber laser sensor was demonstrated in 2014 for refractive index and temperature using a tapered optical fiber structure [42]; both parameters were detected as a single lasing mode was shifted. Additionally, the typical FBG thermal response was improved by combing an FBG and MZI into a ring fiber laser cavity [40]; the MZI was fabricated by using a photonic crystal fiber [57]. Most works mentioned above operated at 1.5 μm ; the few works that operated in the 1 μm region can be found in the literature [58,59]. For example, J. A. Martin-Vela [59] et al. proposed a thin core fiber structure as an SH for curvature detection in a ring fiber laser cavity using an Ytterbium-doped fiber. In addition, Yan Bai et al. demonstrated a temperature fiber laser sensor that operated in a 2 μm region [60]; here, the authors employ a Sagnac interferometer as an SH. The wavelength operation involves some characteristics for practical implementations. For instance, for liquid refractive index sensing application, the absorption coefficients should be considered; here, for a 1.0 μm region, the penetration depth is a few centimeters; in contrast, for 2.0 μm , the penetration depth is less than one millimeter. Moreover, 1.5 μm offers low loss transmission for remote sensing application. The 2.0 μm offers a good absorption coefficient for gas sensing and LiDAR systems. In addition, the technology for detection is commercially available for each wavelength range.

2.2. Brillouin Fiber Laser Sensor

Some fiber laser sensors exploit the stimulated Brillouin scattering (SBS) effect to detect external parameters via frequency/wavelength shifting. The SBS is a nonlinear phenomenon where a high-intensity pump source generates gain for the counterpropagating signal. The typical Brillouin fiber laser sensor is depicted in Figure 2.

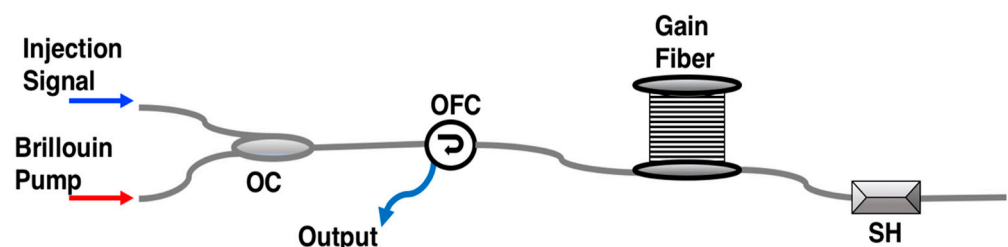


Figure 2. Representative Brillouin fiber laser configuration proposed for sensing.

The Brillouin fiber laser sensor uses a Brillouin pump (BP) and injection signal (IS). The BP needs to be a high-intensity light source; this high-intensity signal generates acoustic phonons, which propagate as an acoustic wave [61–63]. Both signals are combined by an optical fiber coupler (OC) or by cascade arrangement. These signals are launched to the gain fiber using an optical fiber circulator (OFC). After the gain fiber, an SH is used to monitor the external perturbations. The OFC monitors the reflection frequencies generated by the

system. The optical fiber elements involved are similar to those used for CW operation; however, the BP and IS should have unique characteristics. For instance, the BP needs to be a narrow linewidth with less than 5 nm, and the intensity should be related to the optical fiber length interaction. Meanwhile, the IS should be a low-power signal with two orders of magnitude below the BP; here, the IS can be an independent polarization source. The frequencies involved are linked by the acoustic wave (ν_a); here, the interaction of these frequencies is governed by $\nu_{BP} - \nu_{IS} = \nu_a$. The Brillouin scattering frequency (ν_B) can be described as follows [8,62,63]:

$$\nu_B = 2nV_a / \lambda_{BP}$$

where λ_{BP} is the central peak wavelength of the BP, and n is the refractive index of the optical fiber. Considering that the gain fiber length is too long, it is necessary to use an SH.

In 2007, O. Frazão et al. proposed a dual sensor based on SBS [21]. Temperature and strain sensing were achieved with a good resolution ($\pm 1 \mu\epsilon$ and $\pm 1^\circ\text{C}$), and the fiber laser sensor employed an FBG as an SH. It is important to recall that the resolution of the fiber laser sensor depends on the device used to monitor the laser output. Higher resolution can be achieved by an optical spectrum analyzer (OSA) with a typical resolution of 0.02 nm. For instance, the CW fiber laser sensor for temperature and liquid level reported by Weihua Zhang [27] exhibited a resolution of 0.111°C . Multiwavelength Brillouin fiber laser sensors have been demonstrated as strain sensors [64,65]. Additionally, Joseph B. Murray et al. proposed a strain Brillouin fiber laser sensor with the capability to detect minimal dynamic measurement of $4 \text{ n}\epsilon/\text{Hz}^{1/2}$ [66]. As previously mentioned, the resolution is related to the device used to monitor the laser response; however, some techniques can improve the resolution for dynamic measurement [19].

2.3. Mode-Locked Fiber Laser Sensor

In a fiber laser cavity, when the loss signal frequency matches the frequency spacing of the longitudinal modes, the mode-locking effect occurs [9,11]. There are two types of mode-locked fiber lasers: active and passive. The active configurations involve an acoustic-optic or electro-optic modulator, or a semiconductor electro-absorption modulator. This element generates a periodic cavity for loss modulation. In contrast, a saturable absorber element is involved in the passive technique. The fiber laser cavity losses are increased when the light interacts with the absorbing medium. This technique offers a very short pulse. The typical mode-locked fiber laser sensor configurations are shown in Figure 3. Figure 3a shows a ring fiber laser cavity that employs a saturable absorber used to operate as a passive mode-locked laser. A nanomaterial was used as a saturable medium in the fiber laser sensors based on a passive mode-locked operation. The elements involved in the Q-switch ring laser cavity (see Figure 3a) operate similarly to those described in Figure 1a. The saturable absorber material is placed at the facet of an optical fiber terminator then sandwiched by a second optical fiber terminator using an interconnector. The linear laser configuration shown in Figure 3b is an actively mode-locked fiber laser that employs a phase modulator (PM). Here, the light is launched to the cavity by the WDM; then, the light reaches the gain medium. The signal generated by the DOF goes to the PC and the PM modulates its intensity; the cavity is closed by an optical fiber loop ensemble by an OC. An optical mirror ensures the cavity light oscillation.

It is essential to mention that the fiber laser cavities shown in Figure 3 were mostly demonstrated as an optical fiber gyroscope, which is the most common application for mode-locked fiber lasers. However, as discussed below in Sections 3 and 4, these configurations can be used for monitoring temperature and strain. More detailed information about the principle of operation of the mode-locked fiber laser can be found in [67,68].

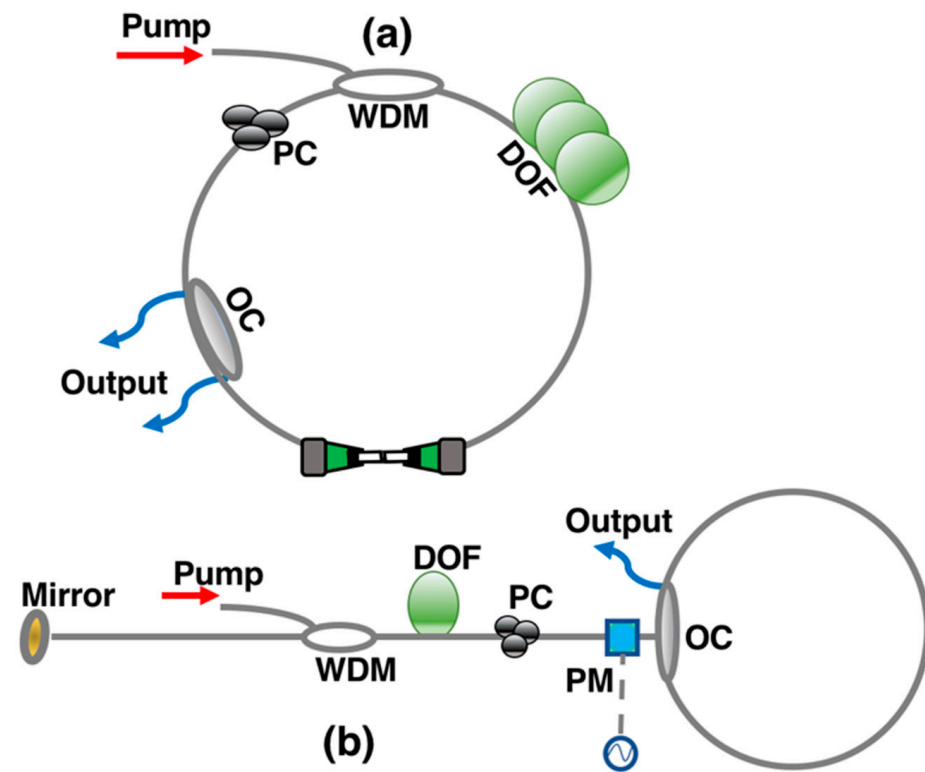


Figure 3. Classical mode-locked fiber laser sensor configurations proposed for sensing. (a) Ring laser configuration based on saturable absorber, here a nanomaterial is set between two fiber optic connectors; and (b) active mode-locked linear laser.

2.4. Distributed-Feedback Fiber Laser Sensor

A distributed-feedback (DFB) fiber laser is an optical fiber with a gain medium and a series of reflectors. The reflectors are usually inscribed inside or close to the gain medium. The typical configuration of a DFB is shown in Figure 4. This fiber laser is composed of a doped optical fiber itself. Here, the pump goes to the FBG, then the signal goes to the doped section, and the amplified spontaneous emission (ASE) signal reaches the second FBG. Both FBGs provide a cavity oscillation, as well as an output laser; however, the high intensity is monitored in reflection mode. Moreover, an optical fiber loop mirror can replace the second FBG.

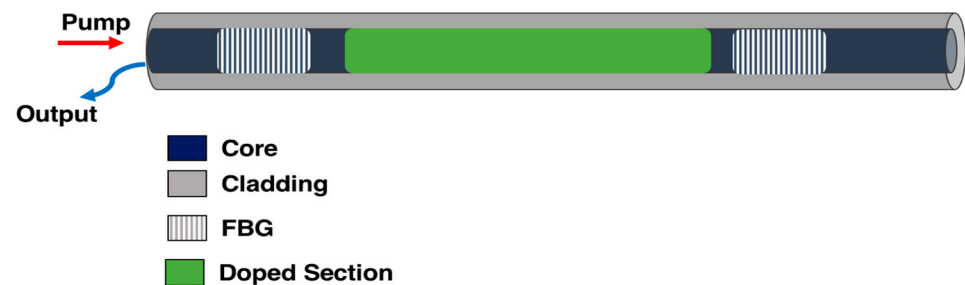


Figure 4. Configuration of distributed-feedback reflector in a fiber laser sensor.

The FBG is the predominant reflector used in a DFB fiber laser sensor. These FBGs offer wavelength and bandwidth selectivity [15]. The frequency value of specific longitudinal mode spacing in a laser cavity is determined by [69,70]:

$$\nu = cN / 2nl$$

where c is the speed of light, N is the number of longitudinal modes, the mode's effective refractive index (n), and the cavity length (l) are the other parameters. The reflection bandwidth generated by the first reflection mode is described by [71]:

$$v_{\lambda_{FBG}} = c\Delta n_{x,y} / \lambda_{FBG}n$$

where, the λ_{FBG} is the Bragg wavelength generated by the reflective index modulation ($\Delta n_{x,y}$) of the reflective index profile of the Bragg grating. The Bragg wavelength is defined by [72]:

$$\lambda_{FBG} = 2n\Lambda$$

where Λ (pitch) represents the distance between both refractive indexes involved in the FBG. Many longitudinal modes are generated by the cavity when the bandwidth of the FBG is much lower than the fundamental frequency. Consequently, if the λ_{FBG} is altered by any physical parameter, the beat frequency of the resonant cavity is altered. This effect has been used for sensing applications.

One of the first approaches to build distributed-feedback fiber laser sensors was proposed by H. K. Kim et al. in 1993 [73]. The authors employ eigenpolarization modes and dichroic mirrors to generate the DFB cavity. A few years later, J. T. Kringlebotn et al. proposed a DFB cavity for pressure and force [72]; here, the authors inscribed an FBG and analyzed the eigenpolarization modes. Li-Yang Shao et al., (2016) demonstrated the simultaneous detection of temperature and strain [74]; both parameters are related to the wavelength and beat frequency, respectively. Other research groups achieved simultaneous detection of temperature and strain by using a phase-shifted FBG in a DFB laser cavity [71].

3. Refractive Index Fiber Laser Sensors

Refractive index (RI) is a crucial parameter in industrial food processing, medical diagnosis, and oil industry. Some research groups have proposed RI fiber laser sensors. As previously mentioned, FBG was one of the first SH used in fiber laser sensor configurations; in 2006, Xiufeng Yang et al. proposed a linear fiber laser cavity based on FBG as a RI sensor [75]. This configuration was improved by modifying the FBG location and integrating optical fiber loops [76]. Furthermore, a microchannel fiber and FBG were integrated into a linear fiber laser cavity for RI sensing [34]. To detect RI, the light into the fiber must interact with the surrounding medium. Then, several optical fiber structures will have been demonstrated for RI sensing [38,77–80]. These structures act as a wavelength selective filter (WSF) into the fiber laser cavity and provide a tunable effect or, in some cases, intensity modulation. Several works employ tapered optical fibers WSF for RI sensing purposes [41,42,77,78,81–83]. Other alternatives employ optical fiber structures with miss-match core sections, then the light that interacts with the surrounding medium is higher and provides attractive characteristics [33,41,79,80,84–89]. For example, Bin Yin et al. propose an FBG and multimode fiber (MMF) integration to detect three parameters, inclusive of RI [38]. The ring laser configuration employs an optical fiber circulator to provide a partial reflector and monitors the MMF-FBG optical fiber structure output, as a result it is possible to discriminate temperature or strain. The ring laser configuration is shown in Figure 5a; for this fiber laser cavity, the elements and principle of operation are similar to those presented in Figure 1c. Another similar fiber laser configuration for monitoring refractive index was proposed by Yuan Cao et al.; the research group proposed a mode-locked fiber laser for refractive index sensing [82] (see Figure 5b). The authors used a ring cavity with a tapered FBG fiber as an SH. The mode-locked effect is excited by several elements such as a Fabry-Perot filter and dispersion medium. This RI sensing configuration achieves a sensitivity of 466.3 $\mu\text{s}/\text{RIU}$. It is essential to notice that this ring fiber laser cavity employs similar elements that are described in Figure 3a; here, the semiconductor optical amplifier (SOA) acts as a gain medium, and the dispersion-shifted fiber (DSF) combined with the Fabry-Perot tunable filter provides an optical frequency scanning filter.

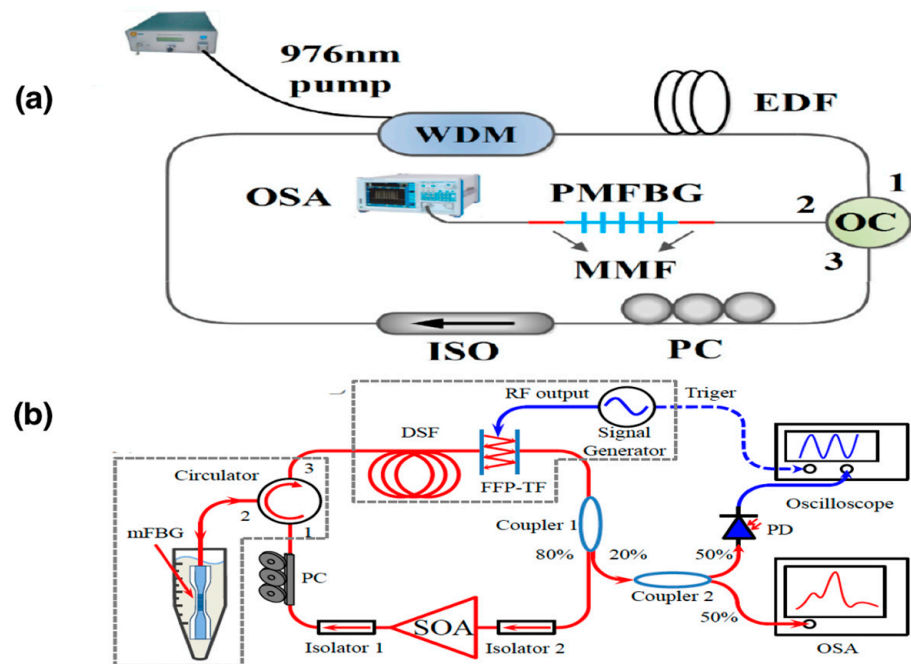


Figure 5. (a) Ring fiber laser sensor cavity and the integration of an FBG operated in reflection mode for RI sensing (reprinted with permission from [38] © The Optical Society); and (b) a mode-locked fiber laser sensor using a tapered fiber as SH for RI (reprinted/adapted with permission from [82] © The Optical Society).

Recently, Weihao Lin et al. achieved an RI ring fiber laser sensor with modest sensitivity close to 150 nm/RIU [81]. Although this sensitivity is not competitive for interferometric fiber optic structures, its demodulation and the ring fiber laser configuration are not intricate (see Figure 6a); moreover, the principle of operation and the elements involve being similar than as previously described in Figure 1a. R. A. Perez-Herrera et al. reported a similar fiber laser configuration for intensity modulation (see Figure 6b) [87]. The authors proposed a ring fiber laser cavity with an FBG by using a 1 × 3 optical fiber coupler, a reference reflection (water and air), and the SH interconnected into the fiber laser cavity. The sensitivity reported was 0.01 nW/RIU. In addition, the principle of operation and elements involved are similar to those previously described in Figure 1c; here, the authors set three reflective devices by a 1 × 3 optical fiber coupler. A few approaches of DFB and mode-locking fiber lasers for refractive index applications can be found in the literature. Xinfeng Yang et al. studied a DFB linear fiber laser cavity for RI and strain [88]; here, the authors polished the DFB to excite light interaction with the surrounding medium; consequently, the authors achieved a sensitivity of 0.1419 GHz/RIU. The fiber laser configuration can be appreciated in Figure 6c. R.I. Álvarez-Tamayo and P. Prieto-Cortes reported a linear fiber laser cavity for refractive index sensing [89]. The linear fiber laser cavity is not intricate, and using a ball lens can estimate the reflective index changes applied at one of the linear fiber laser cavities. The high sensitivity achieved was 1130.28 nm/RIU (see Figure 6d). This cavity is similar than as described in Figure 1d. In Table 1, fiber laser sensors for refractive index are shown regarding sensitivity and fiber laser cavity. It is essential to mention that the sensitivity achieved is strongly related to the equipment used at the laser output. Moreover, intensity and wavelength demodulation imply pros and cons; for instance, intensity demodulation is not intricate; however, power source fluctuations compromise the measurement. In contrast, wavelength demodulation is insensitive to power source variations; however, the demodulation process implies an intricate or expensive stage.

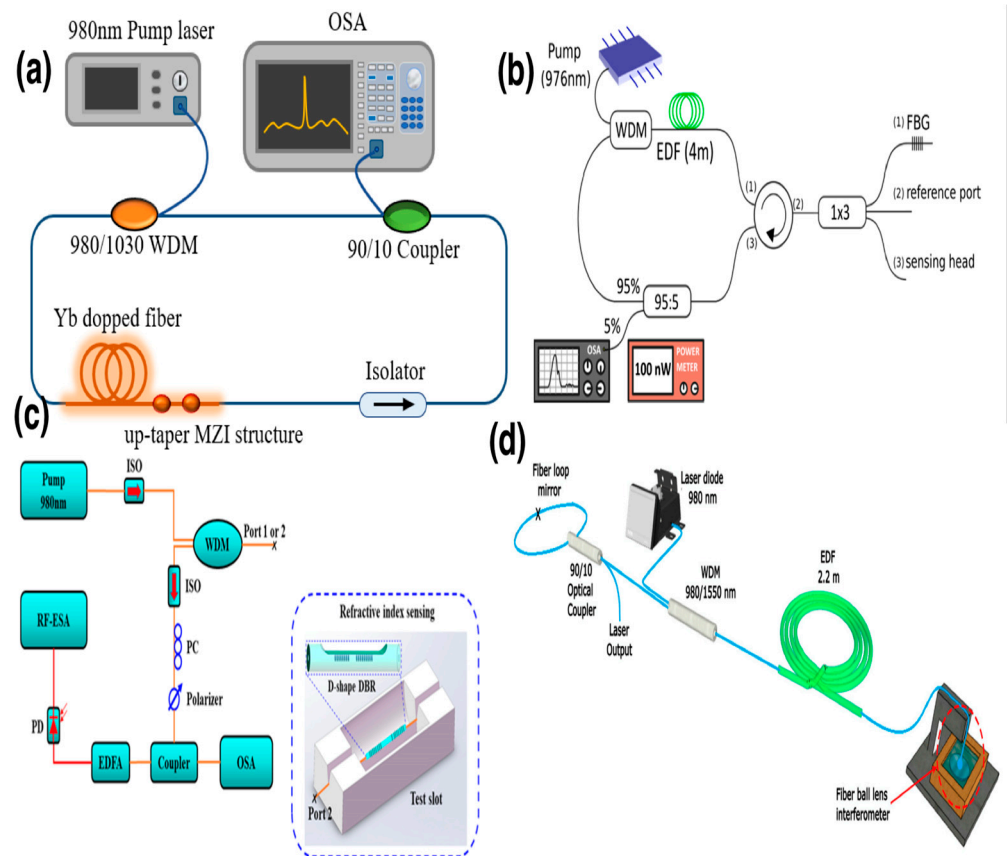


Figure 6. (a) Ring fiber laser sensor configuration for refractive index based on MZI using up-tapers (reprinted from [81], under CC BY 4.0; ©2022 MDPI); (b) ring fiber laser sensor cavity and the integration of an FBG operated in reflection mode for RI sensing (reprinted from [87], under CC BY 4.0; ©2022 MDPI); and (c) a polished DFB as an RI sensor (reprinted/adapted from [88], under CC BY 4.0; ©2019 IEEE) and (d) linear fiber laser sensor cavity for refractive index estimation using a ball-lens as a sensing head (reprinted from [89], under CC BY 4.0; ©2023 MDPI).

Table 1. Comparative table of refractive index fiber laser sensors.

| Fiber Laser Technique | SH | Sensitivity | Gain-Medium | Reference |
|-----------------------|--------------------------|----------------|----------------|-----------|
| CW | Up-taper | 44.8 nm/RIU | Er Doped Fiber | [80] |
| CW | Bend-loop | 60nm/RIU | Er Doped Fiber | [90] |
| CW | Core-offset joint | 52.3 nm/RIU | Er Doped Fiber | [33] |
| CW | No Core Fiber-FBG | 196.1 dB/RIU | Er Doped Fiber | [86] |
| CW | Up-taper-MZI | 151 nm/RIU | Yb Doped Fiber | [81] |
| CW | Taper Fiber | 163.80 nm/RIU | Er Doped Fiber | [42] |
| CW | No Core Fiber | 113.73 dB/RIU | Er Doped Fiber | [86] |
| CW | FBG | 367.9dB/RIU | Er Doped Fiber | [84] |
| CW | Taper Fiber | 549.599 nm/RIU | Tm Doped Fiber | [77] |
| CW | Michelson Interferometer | 1039.77 nm/RIU | Er Doped Fiber | [78] |
| DFB | Polished-DBR | 240.4MHz/RIU | Er Doped Fiber | [91] |
| DFB | Polished-DBR | 0.1419 GHz/RIU | Er Doped Fiber | [88] |
| Mode-locked | Taper Fiber | 466.3 μs/RIU | SOA | [82] |

4. Temperature Fiber Laser Sensors

Temperature is a parameter that can be used in multiple sensing applications for several research fields and industries. Consequently, it is necessary to develop temperature sensors with different temperature ranges and resolutions. Considering the optical fiber properties, it is possible to propose and develop temperature fiber optic sensors with a wide temperature range. The fiber laser sensor characteristics ensure a wide temperature range and good sensing resolution. In 1994, G. A. Ball et al. demonstrated a simple fiber laser configuration based on FBG for temperature detection [7]. Furthermore, Z.Y. Zhang et al. proposed to analyze the fluorescence lifetime in Erbium doped fiber laser sensors to detect very low temperatures (40 K) [92]. Some years later, it was demonstrated that DFB fiber laser cavities can be used to monitor high temperatures; in that work, the authors achieved a wide tunable range using a chirped FBG [93,94]. During that same decade, some groups demonstrated the use of Raman and Brillouin fiber lasers as good temperature fiber optic sensors [21,95]. It is important to mention that the gain medium can be used as a temperature fiber laser sensor by generating a tapered section in the doped fiber [96]. Recently, Koken Fukushima studied the ring fiber laser performance as a temperature sensor using cascaded-chirped long-period fiber grating [97]. Some DFB fiber laser cavities based on FBG as an SH, have been widely demonstrated as reliable devices for simultaneous detection of temperature and strain [93,98]. Furthermore, the FBGs have been integrated into CW ring fiber laser cavities for monitoring temperature [40,58]. It is important to mention that the research community has proposed interesting research, such as SH being proposed for temperature monitoring using CW fiber laser. Another example, A. M. Rodrigues Pinto et al. employed photonic crystal fiber (PCF) into a linear fiber laser cavity and achieved a multiwavelength spectrum, which can be tuned 1 nm in a wide temperature range [99]. Additionally, Xianchao Yang et al. filled a PCF with toluene to achieve a sensitivity close to 1.747 nm/°C; the filled PCF was set into a ring fiber laser cavity configuration [100]. Another alternative for fiber laser sensor was presented by H. Ahmad et al. [101]; here, a ring fiber laser cavity and a photonic filter were integrated for temperature sensing. Filling the SH with isopropanol has also been demonstrated as a reliable alternative to improve the temperature fiber laser sensor performance [102]. Usually, temperature influences other parameters, as a result simultaneous detection is required. Heng Xie et al. reported a Brillouin fiber laser for simultaneous detection of temperature and strain. The configuration employs two SH, with an erbium doped fiber (EDF) used as an SH to monitor temperature; a sensitivity of 0.88 MHz/°C was achieved using the Brillouin frequency [103] (see Figure 7a). This ring fiber laser configuration employs an FBG in reflection mode, and the excitation of SBS; the authors employed an electro-optical modulator (EOM) and tunable laser source (TLS); the laser output was monitored by a photodetector and electronic spectrum analyzer (ESA).

Bin Yin et al. achieved a simultaneous detection of humidity and temperature by using a coated FBG with polyvinyl alcohol; this element was set into a ring fiber laser configuration [104]. This fiber laser offers a thermal sensitivity of 9.1 pm/°C. The fiber laser sensing configuration is shown in Figure 7b. This ring fiber laser employs the element described for Figure 1c. In 2019, the importance of the cross-section's passive fiber used in SBS fiber laser sensors was demonstrated by Sanggwon Song et al. [105]; the authors demonstrated a sensitivity variation of 0.11 MHz/°C using SMF fibers for 1060 nm—with different cross sections. The maximal sensitivity achieved was 1.83 MHz/°C (see Figure 7c). It is important to mention that this linear fiber laser cavity set the fiber under test (FUT) close to the photodetector.

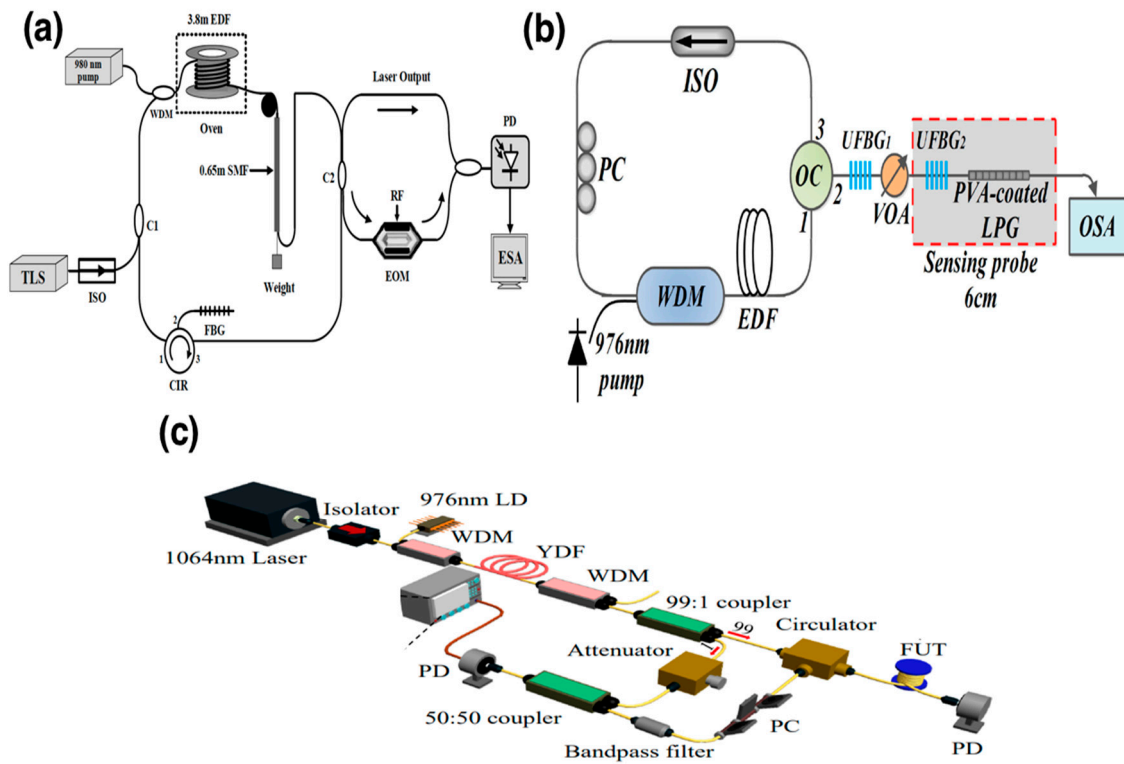


Figure 7. (a) A Brillouin fiber laser temperature-strain sensor (reprinted with permission from [103] © The Optical Society); (b) ring laser humidity-temperature sensor based on coated FBG (reprinted from [104], under CC BY 4.0; ©2020 IEEE); and (c) an SBS fiber laser temperature sensor and its heterodyne demodulation (reprinted and adapted from [105], under CC BY 4.0; ©2019 MDPI).

As previously mentioned, the fiber laser temperature sensitivity can be improved by using isopropanol, this was demonstrated by Weihao Lin et al. [106]. They used a polished fiber as an SH and altered the surrounding media using isopropanol and the SH into a conventional ring fiber laser cavity, showing a thermal sensitivity of 2 nm/°C (see Figure 8a). Here, the refractive index of isopropanol and the vapor pressure change as the temperature is modified; these changes alert the mode coupling in the SH. Another alternative to achieve high thermal sensitivity is by using a cascaded Sagnac interferometer (see Figure 8b). The research group of Liyang Shao achieved a sensitivity of 4.031 nm/°C using this technique in a ring fiber laser cavity [107]. Furthermore, the Sagnac interferometer in a fiber laser cavity allowed a high temperature resolution close to 10⁻⁶ °C [108]. In Table 2, the special characteristics of the temperature fiber laser sensor, as previously discussed, are compared. It is essential to mention that some sensitivities can be compared for CW operation by $f = c/\lambda$, where f is the signal frequency, c is the speed of light, and λ is the wavelength operation. However, it is necessary to consider that the fiber laser should provide a stable single-lasing mode.

Table 2. Temperature fiber laser sensors sensitivity and temperature range comparison.

| Fiber Laser Technique | SH | Sensitivity/ Temperature Range (°C) | Gain Medium | Reference |
|-----------------------|-----|---|----------------|-----------|
| DFB | FBG | 13.38 pm/°C 22–500 | Er Doped Fiber | [93] |
| CW | FBG | 9.7 pm/°C 25–70 | Er Doped Fiber | [109] |

Table 2. Cont.

| Fiber Laser Technique | SH | Sensitivity/ Temperature Range (°C) | Gain Medium | Reference |
|-----------------------|--|---|----------------------------------|-----------|
| CW | Core-offset joint | 44 pm/°C 30–270 | Er Doped Fiber | [110] |
| CW | Sagnac Interferometer | 2 nm/°C 35–31 | Tm Doped Fiber | [61] |
| Raman-Laser | FBG | 30.7 pm/°C 25–55 | Dispersion compensating fiber | [111] |
| EDF/Brillouin Laser | EDF | 1.14 Mhz/°C 25–55 | Er Doped Fiber | [103] |
| CW | Filled Liquid Crystal Hollow Core Fiber | 1.18 nm/°C 22–30 | Er Doped Fiber | [112] |
| CW | Isopropanol Filled optical Coupler | 1.14 nm/°C 20–30 | Er Doped Fiber | [102] |
| CW | Cascaded-Peanut Taper | 571 pm/°C 5–55 | Er Doped Fiber | [113] |
| CW | Fabry-Perot Interferometer | 249 pm/°C 5–55 | Er Doped Fiber | [114] |
| Mode-locked | Long Fiber | 10.27 kHz/°C 30–60 | Er Doped Fiber | [115] |
| Mode-locked | Long Fiber | 44 kHz/°C 20–80 | Er Doped Fiber | [116] |

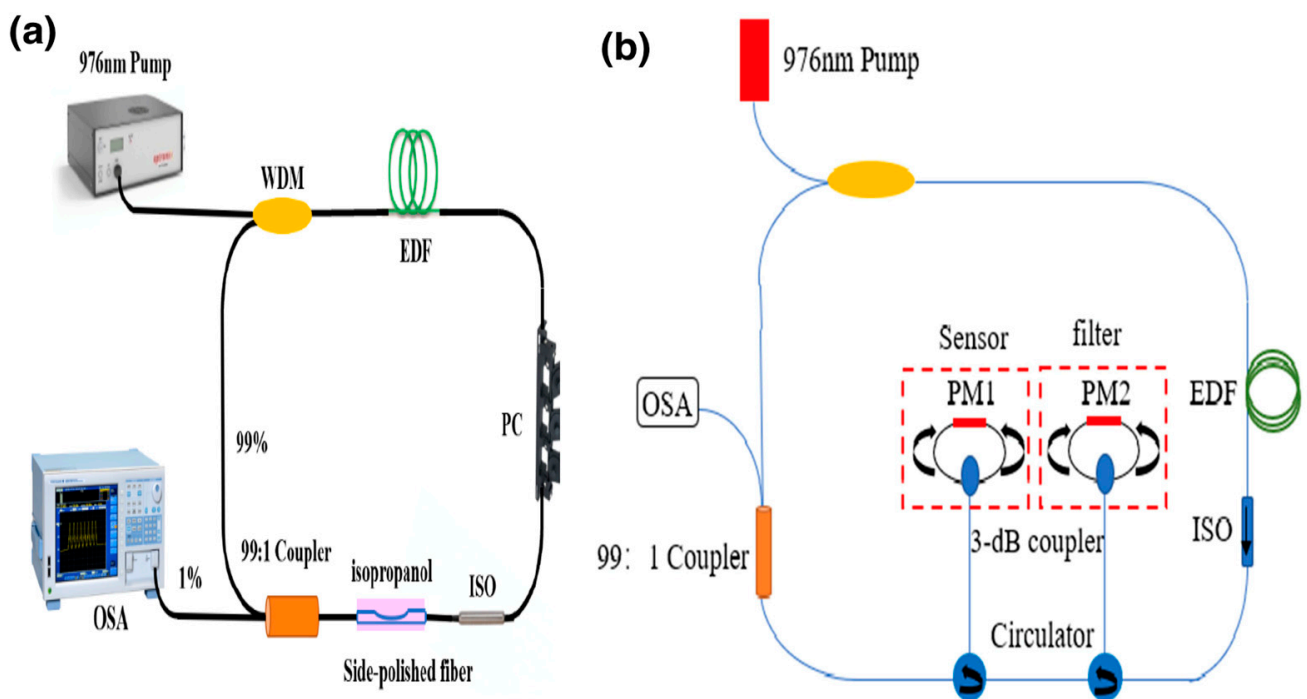


Figure 8. (a) Ring fiber laser cavity using polished fiber immersed in isopropanol for high temperature sensitivity (reprinted from [106], under CC BY 4.0; ©2021 MDPI); and (b) ring fiber laser sensor based on cascade Sagnac interferometers (reprinted from [107], under CC BY 4.0; ©2021 IEEE).

5. Fiber Laser Sensors for Strain Monitoring

At this point, it can be appreciated that strain was one of the first parameters employed to demonstrate fiber laser sensors [13,15,24,117]. Moreover, several fiber laser sensor configurations have been proposed to simultaneously detect strain and other parameters [39,98,103,118–124]. Some fiber laser sensors based on FBG have been demonstrated for pure strain sensing [125,126]. For instance, Zuowei Yin et al. demonstrated that the multiwavelength effect in linear laser configuration could be used to monitor strain with a sensitivity of $\sim 4 \text{ kHz}/\mu\epsilon$ [125]. Additionally, it was demonstrated that a strain fiber laser sensor employing an FBG as an SH, where the authors employed beat frequency demodulation, achieved a maximal sensitivity of $\sim 1.6 \text{ kHz}/\mu\epsilon$ [126]. As previously mentioned, most configurations are sensitive to other parameters. However, H.F. Martins et al. demonstrated a technique insensitive to temperature, linear fiber laser cavity exploited the four-wave mixing effect to detect strain with a sensitivity of $2.3 \text{ pm}/\mu\epsilon$ [127]. Other alternatives with similar sensitivity were reported by [128]; here, the authors employed a multimode interference (MMI) filter as an SH and varied the strain from 0 to $2333 \mu\epsilon$. This sensitivity was improved by Juan Wang et al.; here, the MMI into a linear fiber mode-locked laser improved the sensitivity five times [129]. The linear fiber laser cavity is susceptible to elongation when the strain is applied. Additionally, the lasing modes suffer phase changes by the elastic-optic effect induced by the strain; it is then possible to have a higher sensitivity for specific lasing modes as the strain is applied to the MMI.

An interesting demultiplexed system is proposed in [130], where using a ring laser cavity in a free-running mode and several FBGs can estimate the static strain by the frequency shifting of the multiple lasing modes. According to the results, it is possible to localize the static strain (see Figure 9a). Here, the authors used a mode-locked fiber laser in a free-running laser mode; this cavity is similar to that described in Figure 3a. The authors set an optical fiber coupler to combine the clockwise and anti-clockwise light signals; this signal can localize the strain applied. However, it is important to consider that the most common ring fiber laser sensor configuration operated in CW can be appreciated in Figure 9b; this fiber laser cavity employs the elements described in Figure 1a. In this configuration the strain is applied into the ring laser cavity then a single lasing mode is shifted with a sensitivity of $2.1 \text{ pm}/\mu\epsilon$ [131]. One of the first and most common techniques for pure strain monitoring is shown in Figure 9c. In this cavity, the pump signal (PL) is coupled to gain medium by the WDM; then, the laser spectrum is monitored by an optical fiber coupler; here, one portion is analyzed by the ESA, for temporal response and the rest of the signal is examined by the OSA for wavelength spectrum. This fiber laser configuration was recently improved by Kuikui Guo et al. [118]; here, the authors set a phase-shifted fiber Bragg grating, as a result, they achieved sensitivities of $34.5 \text{ kHz}/\mu\epsilon$ and $1.25 \text{ pm}/\mu\epsilon$ considering the temporal and wavelength spectrum, respectively. The sensitivities and features are compared in Table 3. As previously mentioned, for CW operation, some sensitivities can be compared by $f = c/\lambda$.

Table 3. Fiber laser sensors strain sensitivity comparison.

| Fiber Laser Technique | SH | Sensitivity | Gain Medium | Reference |
|-----------------------|-----------------|-------------------------------|----------------|-----------|
| DFB | FBG | $4 \text{ kHz}/\mu\epsilon$ | Er Doped Fiber | [125] |
| CW | FBG | $1.6 \text{ kHz}/\mu\epsilon$ | Er Doped Fiber | [126] |
| CW | FBG | $1.6 \mu\text{s}/\mu\epsilon$ | Er Doped Fiber | [132] |
| CW | MMI | $2.3 \text{ pm}/\mu\epsilon$ | Er Doped Fiber | [128] |
| CW | Core-offset MZI | $5.2 \text{ pm}/\mu\epsilon$ | Er Doped Fiber | [133] |

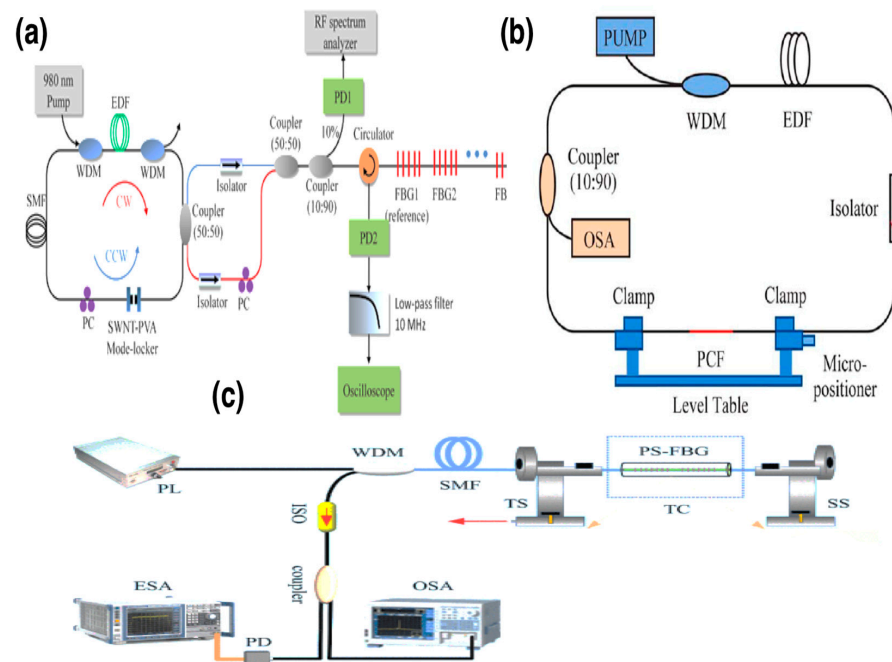


Figure 9. (a) Free-running fiber laser and its multiplexed FBG strain monitoring (reprinted/adapted with permission from [130] © The Optical Society); (b) ring fiber laser cavity for strain monitoring based on photonic crystal fiber (reprinted from [131] with permission ©2014 IEEE); and (c) the most common distributed feedback fiber laser cavity for strain monitoring using the temporal and wavelength spectra (reprinted and adapted from [118], under CC BY 4.0; ©2020 IEEE).

6. Fiber Laser Sensors for Other Parameters

As previously mentioned, several other parameters have been detected using fiber laser cavities. One special application are fiber laser gyroscopes; most of the fiber laser proposed to monitoring rotation are based on Q-switch fiber lasers. Detailed information and discussion about fiber laser gyroscopes can be found in [69,134,135]. Another parameter widely studied for fiber laser sensors are curvature-bending fiber laser sensors; most of the fiber laser configurations previously described can be employed for curvature detection [35,36,60,136,137]. The fiber laser sensors offer the possibility to detect a magnetic field without a special magnetic fluid [46]. This was demonstrated by the Faraday effect in a DBR laser cavity. Another interesting alternative was proven for liquid level, where the SH is sensitive to the liquid surrounding media (same case than RI) and the section covered by the liquid [47]. Gas concentration detection is also an interesting application of fiber laser cavities; to achieve this detection it is important to consider the absorption wavelength for specific gases and cells where the detection is implemented [26,138]. As it can be appreciated, the fiber laser configuration can detect multiple parameters with a simple demodulation process. It is essential to mention that previous efforts have been proposed to discuss the vast capabilities that fiber laser sensors offer. The following references present exciting approaches that cover this interesting device in different forms: [73,139–142].

7. Conclusions

The most representative fiber laser configurations demonstrated and proposed for sensing purposes were discussed. The literature shows that temperature can be detected with a suitable sensitivity while using the most common fiber laser configurations operated in different modes. In addition, the refractive index can be detected by employing these configurations, and the achieved sensitivities are similar to those achieved by interferometric fiber optic sensors. However, fiber laser sensors offer a simple demodulation process. In some cases, the strain fiber laser sensors are competitive with interesting interrogator modes. The fiber laser sensor’s sensitivities are strongly related to the SH characteristics

and its initial sensitivity can be improved with the proper fiber laser cavity configuration. The most common sensing head is the FBG, which can be used in reflection or transmission mode in several fiber laser configurations. This sensing head has a modest sensitivity; however, the fiber laser sensors based on interferometric sensing heads show higher sensitivities. The fiber laser sensors offer wavelength and intensity demodulation operation. The wavelength demodulation offers immunity to power source variation; however, the device to detect the changes is a critical aspect to be considered. Meanwhile, the intensity fiber laser sensor offers no intricate demodulation process. Subsequently, fiber laser sensors offer versatile demodulation processes according to real-life demands.

Author Contributions: Conceptualization, D.J.-V. and J.A.A.-C.; methodology, H.L.O. and J.M.E.-A.; investigation, T.L.-H. and J.M.S.-H.; writing—original draft preparation, D.J.-V. and J.A.A.-C.; writing—review and editing, D.J.-V. and J.A.A.-C.; visualization, J.M.S.-H.; funding acquisition, J.M.E.-A. and H.L.O. All authors have read and agreed to the published version of the manuscript.

Funding: This research was funded by CONACYT grant A1-S-33363/CB2018.

Institutional Review Board Statement: Not applicable.

Informed Consent Statement: Not applicable.

Data Availability Statement: Data sharing not applicable.

Acknowledgments: Completing this review was only possible with the contributions of many research groups devoted to optical fiber lasers.

Conflicts of Interest: The authors declare no conflict of interest.

References

- Maiman, T.H. Stimulated Optical Radiation in Ruby. *Nature* **1960**, *187*, 493–494. [[CrossRef](#)]
- Kissinger, C.D. Fiber Optic Proximity Probe. U.S. Patent 3327584A, 27 June 1967.
- Koester, C.J.; Snitzer, E. Amplification in a Fiber Laser. *Appl. Opt.* **1964**, *3*, 1182–1186. [[CrossRef](#)]
- Payne, D.N. Low-threshold tunable CW and Q-switched fibre laser operating at 1.55 μm . *Electron. Lett.* **1986**, *22*, 159–160.
- Desurvire, E.; Simpson, J.R.; Becker, P.C. High-gain erbium-doped traveling-wave fiber amplifier. *Opt. Lett.* **1987**, *12*, 888–890. [[CrossRef](#)] [[PubMed](#)]
- Alavie, A.T.; Karr, S.E.; Measures, R.M.; Othonos, A. A Multiplexed Bragg Grating Fiber Laser Sensor System. *IEEE Photonics Technol. Lett.* **1993**, *5*, 1112–1114. [[CrossRef](#)]
- Ball, G.A.; Morey, W.W.; Cheo, P.K. Fiber Laser Source/Analyzer for Bragg Grating Sensor Array Interrogation. *J. Light. Technol.* **1994**, *12*, 700–703. [[CrossRef](#)]
- Zarinetchi, F.; Smith, S.P.; Ezekiel, S. Stimulated Brillouin fiber-optic laser gyroscope. *Opt. Lett.* **1991**, *16*, 229–231. [[CrossRef](#)]
- Jeon, M.Y.; Jeong, H.J.; Kim, B.Y. Mode-locked fiber laser gyroscope. *Opt. Lett.* **1993**, *18*, 320. [[CrossRef](#)]
- Kim, H.K.; Park, H.G.; Kim, B.Y.; Kim, S.K. Polarimetric fiber laser sensors. *Opt. Lett.* **1993**, *18*, 317. [[CrossRef](#)]
- Lee, B.W.; Jeong, H.J.; Kim, B.Y. High-sensitivity mode-locked fiber laser gyroscope. *Opt. Lett.* **1997**, *22*, 129. [[CrossRef](#)]
- Dong, X.; Ngo, N.Q.; Shum, P.; Guan, B.-O.; Tam, H.-Y.; Dong, X. Concentration-induced nonuniform power in tunable erbium-doped fiber lasers. *Opt. Lett.* **2004**, *29*, 358. [[CrossRef](#)] [[PubMed](#)]
- Melle, S.M.; Alavie, A.T.; Karr, S.; Coroy, T.; Liu, K.; Measures, R.M. A Bragg grating-tuned fiber laser strain sensor system. *IEEE Photonics Technol. Lett.* **1993**, *5*, 263–266. [[CrossRef](#)] [[PubMed](#)]
- Zhang, Y.; Zhang, M.; Jin, W. Sensitivity enhancement in erbium-doped fiber laser intra-cavity absorption sensor. *Sens. Actuators A Phys.* **2003**, *104*, 183–187. [[CrossRef](#)]
- Cranch, G.A.; Flockhart, G.M.H.; Kirkendall, C.K. Distributed feedback fiber laser strain sensors. *IEEE Sens. J.* **2008**, *8*, 1161–1172. [[CrossRef](#)]
- Ames, G.H.; Maguire, J.M. Erbium fiber laser accelerometer. *IEEE Sens. J.* **2007**, *7*, 557–561. [[CrossRef](#)]
- Frazão, O.; Correia, C.; Baptista, J.M.; Marques, M.B.; Santos, J.L. Ring fibre laser with interferometer based in long period grating for sensing applications. *Opt. Commun.* **2008**, *281*, 5601–5604. [[CrossRef](#)]
- Fu, H.; Shu, X.; Mou, C.; Zhang, L.; He, S.; Bennion, I. Transversal loading sensor based on tunable beat frequency of a dual-wavelength fiber laser. *IEEE Photonics Technol. Lett.* **2009**, *21*, 987–989. [[CrossRef](#)]
- Nakazaki, Y.; Yamashita, S. Fast and wide tuning range wavelength-swept fiber laser based on dispersion tuning and its application to dynamic FBG sensing. *Opt. Express* **2009**, *17*, 8310. [[CrossRef](#)]
- Galindez, C.A.; Madruga, F.J.; Ullan, A.; Lopez-Amo, M.; Lopez-Higuera, J.M. Temperature sensing in multiple zones based on Brillouin fiber ring laser. *J. Phys. Conf. Ser.* **2009**, *178*, 012017. [[CrossRef](#)]

21. Frazão, O.; Marques, J.M.; Santos, J.L.; Marques, M.B.; Baptista, J.M. Brillouin fibre laser discrete sensor for simultaneous strain and temperature measurement. *Appl. Phys. B Lasers Opt.* **2007**, *86*, 555–558. [[CrossRef](#)]
22. Frazão, O. Fiber ring laser sensor for strain-temperature discrimination based on four-wave mixing effect. *Opt. Eng.* **2007**, *46*, 010502. [[CrossRef](#)]
23. Jackson, D.A. High temperature Fabry-Perot probe interrogated with tunable fibre ring laser. *Electron. Lett.* **2008**, *44*, 898–899. [[CrossRef](#)]
24. Xu, O.; Lu, S.; Feng, S.; Jian, S. A novel fiber-laser-based fiber Bragg grating strain sensor with high-birefringence Sagnac fiber loop mirror. *Chin. Opt. Lett.* **2008**, *6*, 818–820. [[CrossRef](#)]
25. Chen, W.; Zhu, H.N.; Man, W.J.; Xiong, S.; Xie, L. Discretely tunable fiber ring laser using FBG tunable filter and Mach-Zehnder interferometer. *Microw. Opt. Technol. Lett.* **2009**, *51*, 2595–2598. [[CrossRef](#)]
26. Zhang, Y.; Zhang, M.; Jin, W.; Ho, H.L.; Demokan, M.S.; Fang, X.H.; Culshaw, B.; Stewart, G. Investigation of erbium-doped fiber laser intra-cavity absorption sensor for gas detection. *Opt. Commun.* **2004**, *234*, 435–441. [[CrossRef](#)]
27. Zhang, W.; Ying, Z.; Yuan, S.; Tong, Z. A fiber laser sensor for liquid level and temperature based on two taper structures and fiber Bragg grating. *Opt. Commun.* **2015**, *342*, 243–246. [[CrossRef](#)]
28. Sun, C.; Dong, Y.; Wang, M.; Jian, S. Liquid level and temperature sensing by using dual-wavelength fiber laser based on multimode interferometer and FBG in parallel. *Opt. Fiber Technol.* **2018**, *41*, 212–216. [[CrossRef](#)]
29. Zhao, Z.Q.; Lu, Y.; Duan, L.C.; Wang, M.T.; Zhang, H.W.; Yao, J.Q. Fiber ring laser sensor based on hollow-core photonic crystal fiber. *Opt. Commun.* **2015**, *350*, 296–300. [[CrossRef](#)]
30. Lopez-Dieguez, Y.; Estudillo-Ayala, J.M.; Jauregui-Vazquez, D.; Herrera-Piad, L.A.; Sierra-Hernandez, J.M.; Garcia-Mina, D.F.; Gallegos-Arellano, E.; Hernandez-Garcia, J.C.; Rojas-Laguna, R. Erbium ring fiber laser cavity based on tip modal interferometer and its tunable multi-wavelength response for refractive index and temperature. *Appl. Sci.* **2018**, *8*, 1337. [[CrossRef](#)]
31. Wang, Z.; Tan, Z.; Xing, R.; Liang, L.; Qi, Y.; Jian, S. Liquid level sensor based on fiber ring laser with single-mode-offset coreless-single-mode fiber structure. *Opt. Laser Technol.* **2016**, *84*, 59–63. [[CrossRef](#)]
32. Shi, J.; Xu, D.; Xu, W.; Wang, Y.; Yan, C.; Zhang, C.; Yan, D.; He, Y.; Tang, L.; Zhang, W.; et al. Humidity Sensor Based on Fabry-Perot Interferometer and Intracavity Sensing of Fiber Laser. *J. Light. Technol.* **2017**, *35*, 4789–4795. [[CrossRef](#)]
33. Xing, R.; Wang, Z.; Gao, Y.; Qi, Y.; Jian, S. RI Ring Laser Sensor Based on Concatenating CLF and SMF with One Core-Offset Joint. *IEEE Photonics Technol. Lett.* **2016**, *28*, 1225–1228. [[CrossRef](#)]
34. Mou, C.; Zhou, K.; Davies, E.; Zhang, L.; Bennion, I. Fiber laser incorporating an intracavity microchannel for refractive index and temperature sensing. *IEEE Photonics Technol. Lett.* **2009**, *21*, 1559–1561. [[CrossRef](#)]
35. Martin-Vela, J.A.; Sierra-Hernandez, J.M.; Martinez-Rios, A.; Estudillo-Ayala, J.M.; Gallegos-Arellano, E.; Toral-Acosta, D.; Porraz-Culebro, T.E.; Jauregui-Vazquez, D. Curvature Sensing Setup Based on a Fiber Laser and a Long-Period Fiber Grating. *IEEE Photonics Technol. Lett.* **2019**, *31*, 1265–1268. [[CrossRef](#)]
36. Sun, C.; Wang, M.; Liu, J.; Ye, S.; Liang, L.; Jian, S. Fiber Ring Cavity Laser Based on Modal Interference for Curvature Sensing. *IEEE Photonics Technol. Lett.* **2016**, *28*, 923–926. [[CrossRef](#)]
37. Othonos, A.; Alavie, A.T.; Melle, S.; Karr, S.E.; Measures, R.M. Fiber Bragg grating laser sensor. *Opt. Eng.* **1993**, *32*, 2841–2846. [[CrossRef](#)]
38. Yin, B.; Wang, M.; Wu, S.; Tang, Y.; Feng, S.; Wu, Y.; Zhang, H. Fiber ring laser based on MMF-PMFBG-MMF filter for three parameters sensing. *Opt. Express* **2017**, *25*, 30946. [[CrossRef](#)]
39. Gao, L.; Chen, L.; Huang, L.; Liu, S.; Yin, Z.; Chen, X. Simultaneous measurement of strain and load using a fiber laser sensor. *IEEE Sens. J.* **2012**, *12*, 1513–1517. [[CrossRef](#)]
40. Gonzalez-Reyna, M.A.; Alvarado-Mendez, E.; Estudillo-Ayala, J.M.; Vargas-Rodriguez, E.; Sosa-Morales, M.E.; Sierra-Hernandez, J.M.; Jauregui-Vazquez, D.; Rojas-Laguna, R. Laser temperature sensor based on a fiber bragg grating. *IEEE Photonics Technol. Lett.* **2015**, *27*, 1141–1144. [[CrossRef](#)]
41. Zhang, J.; Zhang, H.; Dai, W.; Yang, J. Highly discriminative simultaneous measurement of level, refractive index and temperature of liquid by dual-wavelength fiber ring-cavity laser sensor. *Measurement* **2022**, *204*, 112055. [[CrossRef](#)]
42. Liang, L.; Ren, G.; Yin, B.; Peng, W.; Liang, X.; Jian, S. Refractive index and temperature sensor based on fiber ring laser with STCS fiber structure. *IEEE Photonics Technol. Lett.* **2014**, *26*, 2201–2204. [[CrossRef](#)]
43. Yin, Z.; Gao, L.; Liu, S.; Zhang, L.; Wu, F.; Chen, L.; Chen, X. Fiber ring laser sensor for temperature measurement. *J. Light. Technol.* **2010**, *28*, 3403–3408. [[CrossRef](#)]
44. Shi, J.; Wang, Y.; Xu, D.; Zhang, H.; Su, G.; Duan, L.; Yan, C.; Yan, D.; Fu, S.; Yao, J. Temperature Sensor Based on Fiber Ring Laser with Sagnac Loop. *IEEE Photonics Technol. Lett.* **2016**, *28*, 794–797. [[CrossRef](#)]
45. Bai, X.; Yuan, J.; Gu, J.; Wang, S.; Zhao, Y.; Pu, S.; Zeng, X. Magnetic field sensor using fiber ring cavity laser based on magnetic fluid. *IEEE Photonics Technol. Lett.* **2016**, *28*, 115–118. [[CrossRef](#)]
46. Cheng, L.; Han, J.; Jin, L.; Guo, Z.; Guan, B.-O. Sensitivity enhancement of Faraday effect based heterodyning fiber laser magnetic field sensor by lowering linear birefringence. *Opt. Express* **2013**, *21*, 30156. [[CrossRef](#)] [[PubMed](#)]
47. Liang, X.; Liu, Z.; Wei, H.; Li, Y.; Jian, S. Detection of Liquid Level with an MI-Based Fiber Laser Sensor Using Few-Mode EMCF. *IEEE Photonics Technol. Lett.* **2015**, *27*, 805–808. [[CrossRef](#)]
48. Liu, X.; Wang, F.; Yang, J.; Zhang, X.; Du, X. Fiber ring laser directional torsion sensor with ultra-wide linear response. *Sensors* **2019**, *19*, 3613. [[CrossRef](#)]

49. Hong, J.B.; Yeo, Y.B.; Lee, B.W.; Kim, B.Y. Phase sensitive detection for mode-locked fiber laser gyroscope. *IEEE Photonics Technol. Lett.* **1999**, *11*, 1030–1032. [[CrossRef](#)]
50. Yang, X.; Duan, L.; Zhang, H.; Lu, Y.; Wang, G.; Yao, J. Highly sensitive dual-wavelength fiber ring laser sensor for the low concentration gas detection. *Sens. Actuators B Chem.* **2019**, *296*, 126637. [[CrossRef](#)]
51. Shi, J.; Wang, Y.; Xu, D.; He, Y.; Jiang, J.; Xu, W.; Zhang, H.; Su, G.; Yan, C.; Yan, D.; et al. Remote Gas Pressure Sensor Based on Fiber Ring Laser Embedded with Fabry-Pérot Interferometer and Sagnac Loop. *IEEE Photonics J.* **2016**, *8*, 6804408. [[CrossRef](#)]
52. Meng, D.; Zhang, X.; Wang, D.; Miao, C.; Shi, J.; Li, X.; Bai, H.; Chen, H.; Guo, C.; Yao, J. Gas Pressure Sensor with Low Detection Limit Based on Fabry-Perot Interferometer and Intracavity Sensing of Fiber Ring Laser. *IEEE Sens. J.* **2022**, *22*, 6606–6611. [[CrossRef](#)]
53. Mađry, M.; Alwis, L.; Binetti, L.; Pajewski, L.; Bereś-Pawlik, E. Simultaneous Measurement of Temperature and Relative Humidity Using a Dual-Wavelength Erbium-Doped Fiber Ring Laser Sensor. *IEEE Sens. J.* **2019**, *19*, 9215–9220. [[CrossRef](#)]
54. Fan, H.; Chen, L.; Bao, X. Fiber-Optic Sensor Based on Core-Offset Fused Unequal-Length Fiber Segments to Improve Ultrasound Detection Sensitivity. *IEEE Sens. J.* **2020**, *20*, 9148–9154. [[CrossRef](#)]
55. Bellemare, A.; Karásek, M.; Riviere, C.; Babin, F.; He, G.; Roy, V.; Schinn, G.W. A broadly tunable erbium-doped fiber ring laser: Experimentation and modeling. *IEEE J. Sel. Top. Quantum Electron.* **2001**, *7*, 22–29. [[CrossRef](#)]
56. Paschotta, R.; Nilsson, J.; Reekie, L.; Trooper, A.C.; Hanna, D.C. Single-frequency ytterbium-doped fiber laser stabilized by spatial hole burning. *Opt. Lett.* **1997**, *22*, 40. [[CrossRef](#)]
57. Sierra-Hernandez, J.M.; Rojas-Laguna, R.; Vargas-Rodriguez, E.; Estudillo-Ayala, J.M.; Jauregui-Vazquez, D.; Guzmán-Chávez, A.D.; Zaca-Moran, P. A tunable multi-wavelength erbium doped fiber laser based on a Mach-Zehnder interferometer and photonic crystal fiber. *Laser Phys.* **2013**, *23*, 125103. [[CrossRef](#)]
58. Merza, H.Q.; Al-Hayali, S.K.; Al-Janabi, A.H. All-fiber Mach-Zehnder interferometric comb filter based on macrobend single-mode optical fiber for selecting lasing performance in 1-micron region. *Opt. Commun.* **2021**, *493*, 127017. [[CrossRef](#)]
59. Martin-Vela, J.A.; Sierra-Hernandez, J.M.; Jauregui-Vazquez, D.; Estudillo-Ayala, J.M.; Hernandez-Garcia, J.C.; Reyes-Ayona, J.R.; Garcia-Mina, D.F.; Rojas-Laguna, R. Highly Sensitive Fiber Ring Laser Sensor for Curvature Using a Modal Interferometer. *IEEE Sens. J.* **2020**, *20*, 9864–9870. [[CrossRef](#)]
60. Bai, Y.; Yan, F.; Feng, T.; Han, W.; Zhang, L.; Cheng, D.; Bai, Z.; Wen, X. Temperature fiber sensor based on single longitudinal mode fiber laser in 2 μm band with Sagnac interferometer. *Opt. Fiber Technol.* **2019**, *51*, 71–76. [[CrossRef](#)]
61. Smith, S.P.; Zarinetchi, F.; Ezekiel, S. Narrow-linewidth stimulated Brillouin fiber laser and applications. *Opt. Lett.* **1991**, *16*, 393. [[CrossRef](#)]
62. Harun, S.W.; Shirazi, M.R.; Ahmad, H. Multiple wavelength Brillouin fiber laser from injection of intense signal light. *Laser Phys. Lett.* **2007**, *4*, 678–680. [[CrossRef](#)]
63. Kotlicki, O.; Scheuer, J.; Shahriar, M.S. Theoretical study on Brillouin fiber laser sensor based on white light cavity. *Opt. Express* **2012**, *20*, 28234. [[CrossRef](#)] [[PubMed](#)]
64. Liu, Y.; Zhang, M.; Wang, P.; Li, L.; Wang, Y.; Bao, X. Multiwavelength Single-Longitudinal-Mode Brillouin-Erbium Fiber Laser Sensor for Temperature Measurements with Ultrahigh Resolution. *IEEE Photonics J.* **2015**, *7*, 6802809. [[CrossRef](#)]
65. Murray, J.B.; Cerjan, A.; Redding, B. Distributed Brillouin fiber laser sensor. *Optica* **2022**, *9*, 80. [[CrossRef](#)]
66. Wang, Y.; Xu, C.Q. Actively Q-switched fiber lasers: Switching dynamics and nonlinear processes. *Prog. Quantum Electron.* **2007**, *31*, 131–216. [[CrossRef](#)]
67. Ippen, E.P. Principles of passive mode locking. *Appl. Phys. B Laser Opt.* **1994**, *58*, 159–170. [[CrossRef](#)]
68. Rønnekleiv, E.; Ibsen, M.; Zervas, M.N.; Laming, R.I. Characterization of fiber distributed-feedback lasers with an index-perturbation method. *Appl. Opt.* **1999**, *38*, 4558. [[CrossRef](#)]
69. Liu, Y.; Zhang, W.; Xu, T.; He, J.; Zhang, F.; Li, F. Fiber laser sensing system and its applications. *Photonic Sens.* **2011**, *1*, 43–53. [[CrossRef](#)]
70. Hadelier, O.; Ibsen, M.; Zervas, M.N. Distributed-feedback fiber laser sensor for simultaneous strain and temperature measurements operating in the radio-frequency domain. *Appl. Opt.* **2001**, *40*, 3169. [[CrossRef](#)]
71. Kringlebotn, J.T.; Loh, W.H.; Laming, R.I. Polarimetric Er^{3+} -doped fiber distributed-feedback laser sensor for differential pressure and force measurements. *Opt. Lett.* **1996**, *21*, 1869. [[CrossRef](#)]
72. Kim, H.K.; Kim, S.K.; Kim, B.Y. Polarization control of polarimetric fiber-laser sensors. *Opt. Lett.* **1993**, *18*, 1465. [[CrossRef](#)]
73. Shao, L.Y.; Liang, J.; Zhang, X.; Pan, W.; Yan, L. High-resolution refractive index sensing with dual-wavelength fiber laser. *IEEE Sens. J.* **2016**, *16*, 8463–8467. [[CrossRef](#)]
74. Yang, X.; Luo, S.; Chen, Z.; Ng, J.H. Refractive index sensor based on fiber laser. *Microw. Opt. Technol. Lett.* **2007**, *49*, 916–918. [[CrossRef](#)]
75. Arellano-Sotelo, H.; Barmenkov, Y.O.; Kir'yanov, A.V. The use of erbium fiber laser relaxation frequency for sensing refractive index and solute concentration of aqueous solutions. *Laser Phys. Lett.* **2008**, *5*, 825–829. [[CrossRef](#)]
76. Wang, Y.; Chen, Z.; Chen, W.; Zhang, X. Refractive index and temperature sensor based on fiber ring laser with tapered seven core fiber structure in 2 μm band. *Opt. Fiber Technol.* **2021**, *61*, 102388. [[CrossRef](#)]
77. Lin, W.; Zhou, S.; Shao, L.Y.; Vai, M.I.; Shum, P.P.; Zhao, F.; Liu, S.; Hu, J.; Liu, Y. In-Fiber Mach-Zehnder Interferometer Based on Er Doped Up-Taper and Peanut-Shaped Fiber Structure in Fiber Ring Laser. *IEEE Access* **2021**, *9*, 128126–128132. [[CrossRef](#)]

78. Hu, X.-g.; Zhao, Y.; Peng, Y.; Tong, R.-j.; Zheng, H.-k.; Zhao, J.; Hu, S. In-fiber optofluidic michelson interferometer for detecting small volume and low concentration chemicals with a fiber ring cavity laser. *Sens. Actuators B Chem.* **2022**, *370*, 132467. [[CrossRef](#)]
79. Cai, L.; Zhao, Y.; Li, X. gang A fiber ring cavity laser sensor for refractive index and temperature measurement with core-offset modal interferometer as tunable filter. *Sens. Actuators B Chem.* **2017**, *242*, 673–678. [[CrossRef](#)]
80. Zhao, Y.; Cai, L.; Li, X.G. In-Fiber Mach-Zehnder Interferometer Based on Up-Taper Fiber Structure with Er³⁺ Doped Fiber Ring Laser. *J. Light. Technol.* **2016**, *34*, 3475–3481. [[CrossRef](#)]
81. Lin, W.; Liu, Y.; Shum, P.P.; Shao, L. In-Line Mach Zehnder Interferometer Based on Ytterbium Doped Fiber with Up-Taper Structure in Fiber Ring Laser and Its Application in Sensing. *Sensors* **2022**, *22*, 9196. [[CrossRef](#)]
82. Cao, Y.; Wang, L.; Lu, Z.; Wang, G.; Wang, X.; Ran, Y.; Feng, X.; Guan, B. High-speed refractive index sensing system based on Fourier domain mode locked laser. *Opt. Express* **2019**, *27*, 7988. [[CrossRef](#)]
83. Liu, J.; Wang, M.; Liang, X.; Dong, Y.; Xiao, H.; Jian, S. Erbium-doped fiber ring laser based on few-mode-singlemode-few-mode fiber structure for refractive index measurement. *Opt. Laser Technol.* **2017**, *93*, 74–78. [[CrossRef](#)]
84. Yin, B.; Wu, S.; Wang, M.; Liu, W.; Li, H.; Wu, B.; Wang, Q. High-sensitivity refractive index and temperature sensor based on cascaded dual-wavelength fiber laser and SNHNS interferometer. *Opt. Express* **2019**, *27*, 252. [[CrossRef](#)]
85. Zhao, J.; Wang, J.; Zhang, C.; Guo, C.; Bai, H.; Xu, W.; Chen, L.; Miao, C. Refractive Index Fiber Laser Sensor by Using Tunable Filter Based on No-Core Fiber. *IEEE Photonics J.* **2016**, *8*, 6805008. [[CrossRef](#)]
86. Shi, J.; Wang, Y.; Xu, D.; Liu, T.; Xu, W.; Zhang, C.; Yan, C.; Yan, D.; Tang, L.; He, Y.; et al. Temperature Self-Compensation High-Resolution Refractive Index Sensor Based on Fiber Ring Laser. *IEEE Photonics Technol. Lett.* **2017**, *29*, 1743–1746. [[CrossRef](#)]
87. Perez-Herrera, R.A.; Soares, L.; Silva, S.; Frazão, O. Ring Cavity Erbium-Doped Fiber for Refractive Index Measurements. *Sensors* **2022**, *22*, 9315. [[CrossRef](#)] [[PubMed](#)]
88. Yang, X.; Bandyopadhyay, S.; Shao, L.Y.; Xiao, D.; Gu, G.; Song, Z. Side-Polished DBR Fiber Laser with Enhanced Sensitivity for Axial Force and Refractive Index Measurement. *IEEE Photonics J.* **2019**, *11*, 7101910. [[CrossRef](#)]
89. Álvarez-Tamayo, R.I.; Prieto-Cortés, P. Refractive Index Fiber Laser Sensor by Using a Fiber Ball Lens Interferometer with Adjustable Free Spectral Range. *Sensors* **2023**, *23*, 3045. [[CrossRef](#)]
90. Zhang, X.; Liu, Z.; Xie, L.; Peng, W. Refractive Index Sensor Based on Fiber Ring Laser. *IEEE Photonics Technol. Lett.* **2016**, *28*, 524–527. [[CrossRef](#)]
91. Li, M.M.; Liu, B.; Liang, Y.Z.; Liang, H.; Li, J.; Guan, B.O. Refractive Index Detection Based on Beat-frequency of Cladding-carved DBR Fiber Lasers. *Guangzi Xuebao/Acta Photonica Sin.* **2017**, *46*, 15–17. [[CrossRef](#)]
92. Zhang, Z.Y.; Sun, T.; Grattan, K.T.V.; Palmer, A.W. Erbium-doped intrinsic fiber sensor for cryogenic temperature measurement. *Sens. Actuators A Phys.* **1998**, *71*, 183–186. [[CrossRef](#)]
93. Mandal, J.; Shen, Y.; Pal, S.; Sun, T.; Grattan, K.T.V.; Augousti, A.T. Bragg grating tuned fiber laser system for measurement of wider range temperature and strain. *Opt. Commun.* **2005**, *244*, 111–121. [[CrossRef](#)]
94. Mandal, J.; Pal, S.; Sun, T.; Grattan, K.T.V.; Augousti, A.T.; Wade, S.A. Bragg Grating-Based Fiber-Optic Laser Probe for Temperature Sensing. *IEEE Photonics Technol. Lett.* **2004**, *16*, 218–220. [[CrossRef](#)]
95. Han, Y.-G.; Tran, T.V.A.; Kim, S.-H.; Lee, S.B. Multiwavelength Raman-fiber-laser-based long-distance remote sensor for simultaneous measurement of strain and temperature. *Opt. Lett.* **2005**, *30*, 1282. [[CrossRef](#)]
96. Alvarez-Chavez, J.A. Modeling of temperature sensitivity on tapered Yb-doped fiber lasers. *Opt. Eng.* **2012**, *51*, 074203. [[CrossRef](#)]
97. Fukushima, K.; Wada, A.; Tanaka, S.; Ito, F. EDF laser temperature sensor using double-pass cascaded-chirped long-period fiber grating in sigma-cavity configuration. *Opt. Commun.* **2022**, *508*, 127713. [[CrossRef](#)]
98. Gao, L.; Huang, L.; Chen, L.; Chen, X. Simultaneous measurement of strain and temperature with a multi-longitudinal mode erbium-doped fiber laser. *Opt. Commun.* **2013**, *297*, 98–101. [[CrossRef](#)]
99. Pinto, A.M.R.; Lopez-Amo, M.; Kobelke, J.; Schuster, K. Temperature Fiber laser sensor based on a hybrid cavity and a random mirror. *J. Light. Technol.* **2012**, *30*, 1168–1172. [[CrossRef](#)]
100. Yang, X.; Lu, Y.; Liu, B.; Yao, J. Fiber Ring Laser Temperature Sensor Based on Liquid-Filled Photonic Crystal Fiber. *IEEE Sens. J.* **2017**, *17*, 6948–6952. [[CrossRef](#)]
101. Ahmad, H.; Zulkhairi, A.S.; Azzuhri, S.R. Temperature sensor and fiber laser based on optical microfiber knot resonator. *Optik* **2018**, *154*, 294–302. [[CrossRef](#)]
102. Lin, W.; Hu, J.; Zhao, F.; Sun, S.; Liu, Y.; Liu, S.; Yu, F.; Mak, P.U.; Pun, S.H.; Shum, P.P.; et al. Adaptive Fiber-Ring Lasers Based on Isopropanol Filled Microfiber Coupler for High-Sensitivity Temperature Sensing. *Micromachines* **2022**, *13*, 1697. [[CrossRef](#)] [[PubMed](#)]
103. Xie, H.; Sun, J.; Feng, D. Simultaneous measurement of strain and temperature based on hybrid EDF/Brillouin laser. *Opt. Express* **2016**, *24*, 11475. [[CrossRef](#)] [[PubMed](#)]
104. Yin, B.; Sang, G.; Yan, R.; Wu, Y.; Wu, S.; Wang, M.; Liu, W.; Li, H.; Wang, Q. Wavelength-and Intensity-Modulated Dual-Wavelength Fiber Laser Sensor for Simultaneous RH and Temperature Detection. *IEEE Access* **2020**, *8*, 52091–52099. [[CrossRef](#)]
105. Song, S.; Jung, A.; Oh, K. High-temperature sensitivity in stimulated brillouin scattering of 1060 nm single-mode fibers. *Sensors* **2019**, *19*, 4731. [[CrossRef](#)] [[PubMed](#)]
106. Lin, W.; Liu, Y.; Shao, L.; Vai, M.I. A fiber ring laser sensor with a side polished evanescent enhanced fiber for highly sensitive temperature measurement. *Micromachines* **2021**, *12*, 586. [[CrossRef](#)]

107. Lin, W.; Shao, L.; Yibin, L.; Bandyopadhyay, S.; Yuhui, L.; Weijie, X.; Shuaiqi, L.; Jie, H.; Vai, M.I. Temperature Sensor Based on Fiber Ring Laser with Cascaded Fiber Optic Sagnac Interferometers. *IEEE Photonics J.* **2021**, *13*, 2–11. [[CrossRef](#)]
108. Shi, J.; Yang, F.; Xu, W.; Xu, D.; Bai, H.; Guo, C.; Wu, Y.; Zhang, S.; Liu, T.; Yao, J. High-Resolution Temperature Sensor Based on Intracavity Sensing of Fiber Ring Laser. *J. Light. Technol.* **2020**, *38*, 2010–2014. [[CrossRef](#)]
109. Diaz, S.; Lopez-Amo, M. Multiwavelength operation of erbium-doped fiber-ring laser for temperature measurements. *Opt. Laser Technol.* **2016**, *78*, 134–138. [[CrossRef](#)]
110. Hao, X.; Tong, Z.; Zhang, W.; Cao, Y. A fiber laser temperature sensor based on SMF core-offset structure. *Opt. Commun.* **2015**, *335*, 78–81. [[CrossRef](#)]
111. Frazo, O.; Correia, C.; Santos, J.L.; Baptista, J.M. Raman fibre Bragg-grating laser sensor with cooperative Rayleigh scattering for strain-temperature measurement. *Meas. Sci. Technol.* **2009**, *20*, 045203. [[CrossRef](#)]
112. Lin, W.; Zhou, S.; Liu, Y.; Vai, M.I.; Shao, L. Liquid crystal-embedded hollow core fiber temperature sensor in fiber ring laser. *Appl. Sci.* **2021**, *11*, 7103. [[CrossRef](#)]
113. Lin, W.; Zhao, F.; Shao, L.Y.; Vai, M.I.; Shum, P.P.; Sun, S. Temperature Sensor Based on Er-Doped Cascaded-Peanut Taper Structure In-Line Interferometer in Fiber Ring Laser. *IEEE Sens. J.* **2021**, *21*, 21594–21599. [[CrossRef](#)]
114. Zou, H.; Ma, L.; Xiong, H.; Zhang, Y.; Li, Y.T. Fiber ring laser sensor based on Fabry-Perot cavity interferometer for temperature sensing. *Laser Phys.* **2018**, *28*, 015102. [[CrossRef](#)]
115. Luo, J.; Cai, X.; Wang, H.; Fu, H. Temperature sensing technique by using a microwave photonics filter based on an actively mode-locked fiber laser. *Microw. Opt. Technol. Lett.* **2021**, *63*, 2535–2540. [[CrossRef](#)]
116. Luo, J.; Wang, H.; Cai, X.; Luo, Z.; Fu, H. Temperature-sensing scheme based on a passively mode-locked fiber laser via beat frequency demodulation. *Chin. Opt. Lett.* **2023**, *21*, 20603. [[CrossRef](#)]
117. Yang, X.; Luo, S.; Chen, Z.; Ng, J.H.; Lu, C. Fiber Bragg grating strain sensor based on fiber laser. *Opt. Commun.* **2007**, *271*, 203–206. [[CrossRef](#)]
118. Guo, K.; He, J.; Xu, G.; Wang, Y. Dual-polarization distributed feedback fiber laser sensor based on femtosecond laser-inscribed in-fiber stressors for simultaneous strain and temperature measurements. *IEEE Access* **2020**, *8*, 97823–97829. [[CrossRef](#)]
119. Gao, L.; Chen, L.; Huang, L.; Chen, X. Multimode fiber laser for simultaneous measurement of strain and temperature based on beat frequency demodulation. *Opt. Express* **2012**, *20*, 22517. [[CrossRef](#)]
120. Yu, K.; Wu, C.; Sun, M.; Lu, C.; Tam, H.Y.; Zhao, Y.; Shao, L. Fiber laser sensor for simultaneously axial strain and transverse load detection. *Measurement* **2015**, *62*, 137–141. [[CrossRef](#)]
121. Kang, Z.; Sun, J.; Bai, Y.; Jian, S. Twin-Core Fiber-Based Erbium-Doped Fiber Laser Sensor for Decoupling Measurement of Temperature and Strain. *IEEE Sens. J.* **2015**, *15*, 6828–6832. [[CrossRef](#)]
122. Liu, D.; Ngo, N.Q.; Tjin, S.C.; Dong, X. A dual-wavelength fiber laser sensor system for measurement of temperature and strain. *IEEE Photonics Technol. Lett.* **2007**, *19*, 1148–1150. [[CrossRef](#)]
123. Tan, Y.-N.; Zhang, Y.; Jin, L.; Guan, B.-O. Simultaneous strain and temperature fiber grating laser sensor based on radio-frequency measurement. *Opt. Express* **2011**, *19*, 20650. [[CrossRef](#)] [[PubMed](#)]
124. Sanchez-Gonzalez, A.; Perez-Herrera, R.A.; Roldan-Varona, P.; Duran-Escudero, M.; Rodriguez-Cobo, L.; Lopez-Higuera, J.M.; Lopez-Amo, M. A Dual-Wavelength Fiber Laser Sensor with Temperature and Strain Discrimination. *Sensors* **2022**, *22*, 6888. [[CrossRef](#)] [[PubMed](#)]
125. Yin, Z.; Liu, S.; Zhang, L.; Gao, L.; Chen, X. Studies on multi-wavelength fiber Bragg grating laser strain sensor. *Opt. Commun.* **2010**, *283*, 4996–4999. [[CrossRef](#)]
126. Tian, J.; Hou, M.-j.; Jiang, Y.; Luo, H.; Tang, C.-y. Fiber ring laser cavity for strain sensing via beat frequency demodulation. *Opt. Commun.* **2020**, *476*, 126326. [[CrossRef](#)]
127. Martins, H.F.; Marques, M.B.; Frazão, O. Temperature-insensitive strain sensor based on four-wave mixing using Raman fiber Bragg grating laser sensor with cooperative Rayleigh scattering. *Appl. Phys. B Lasers Opt.* **2011**, *104*, 957–960. [[CrossRef](#)]
128. Liu, Z.B.; Li, Y.; Liu, Y.; Tan, Z.W.; Jian, S. A static axial strain fiber ring cavity laser sensor based on multi-modal interference. *IEEE Photonics Technol. Lett.* **2013**, *25*, 2050–2053. [[CrossRef](#)]
129. Wang, J.; Ge, S.; Ren, H.; Huang, T.; Yang, P.; Xu, P.; Bai, S.; Dai, S.; Du, J.; Nie, Q. High-sensitivity micro-strain sensing using a broadband wavelength-tunable thulium-doped all-fiber structured mode-locked laser. *Opt. Lett.* **2022**, *47*, 34. [[CrossRef](#)]
130. Guo, J.; Ding, Y.; Xiao, X.; Kong, L.; Yang, C. Multiplexed static FBG strain sensors by dual-comb spectroscopy with a free running fiber laser. *Opt. Express* **2018**, *26*, 16147–16154. [[CrossRef](#)]
131. Bai, X.; Fan, D.; Wang, S.; Pu, S.; Zeng, X. Strain Sensor Based on Fiber Ring Cavity Laser with Photonic Crystal Fiber In-Line Mach-Zehnder Interferometer. *IEEE Photonics J.* **2014**, *6*, 6801608. [[CrossRef](#)]
132. Guo, W.; Lu, F.; Luo, S.; Yang, X.; Zhou, X.; Lu, C. Interrogation of fiber Bragg grating sensor based on Er-doped fiber laser. *Microw. Opt. Technol. Lett.* **2006**, *48*, 1904–1907. [[CrossRef](#)]
133. Contreras-Teran, M.A.; Jauregui-Vazquez, D.; Gallegos-Arellano, E.; Rojas-Laguna, R.; Reyes-Ayona, J.R.; Estudillo-Ayala, J.M.; Hernandez-Garcia, J.C.; Sierra-Hernandez, J.M. High-resolution strain fiber laser-sensor based on core-offset mach-zehnder interferometer. *Meas. Sci. Technol.* **2023**, *34*, 55202. [[CrossRef](#)]
134. Kudelin, I.; Sugavanam, S.; Chernysheva, M. Rotation active sensors based on ultrafast fibre lasers. *Sensors* **2021**, *21*, 3530. [[CrossRef](#)]

135. Zhang, W.; Xian, T.; Wang, W.; Zhan, L. Advancement and expectations for mode-locked laser gyroscopes. *J. Opt. Soc. Am. B* **2022**, *39*, 3159. [[CrossRef](#)]
136. Xiong, H.; Xu, B.; Wang, D.N. Temperature Insensitive Optical Fiber Laser Bend Sensor with a Low Detection Limit. *IEEE Photonics Technol. Lett.* **2015**, *27*, 2599–2602. [[CrossRef](#)]
137. Álvarez-Tamayo, R.I.; Durán-Sánchez, M.; Prieto-Cortés, P.; Salceda-Delgado, G.; Castillo-Guzmán, A.A.; Selvas-Aguilar, R.; Ibarra-Escamilla, B.; Kuzin, E.A. All-fiber laser curvature sensor using an in-fiber modal interferometer based on a double clad fiber and a multimode fiber structure. *Sensors* **2017**, *17*, 2744. [[CrossRef](#)]
138. Martín-Vela, J.A.; Gallegos-Arellano, E.; Sierra-Hernández, J.M.; Estudillo-Ayala, J.M.; Jauregui-Vázquez, D.; Avila-García, M.S.; Ramírez-Gasca, H.; Rojas-Laguna, R. All single-mode-fiber supercontinuum source setup for monitoring of multiple gases applications. *Sensors* **2020**, *20*, 3239. [[CrossRef](#)]
139. Chen, H.; Gao, S.; Zhang, M.; Zhang, J.; Qiao, L.; Wang, T.; Gao, F.; Hu, X.; Li, S.; Zhu, Y. Advances in random fiber lasers and their sensing application. *Sensors* **2020**, *20*, 6122. [[CrossRef](#)]
140. Fu, H.; Chen, D.; Cai, Z. Fiber sensor systems based on fiber laser and microwave photonic technologies. *Sensors* **2012**, *12*, 5395–5419. [[CrossRef](#)]
141. Shi, W.; Fang, Q.; Zhu, X.; Norwood, R.A.; Peyghambarian, N. Fiber lasers and their applications [Invited]. *Appl. Opt.* **2014**, *53*, 6554–6568. [[CrossRef](#)]
142. Addanki, S.; Amiri, I.S.; Yupapin, P. Review of optical fibers-introduction and applications in fiber lasers. *Results Phys.* **2018**, *10*, 743–750. [[CrossRef](#)]

Disclaimer/Publisher’s Note: The statements, opinions and data contained in all publications are solely those of the individual author(s) and contributor(s) and not of MDPI and/or the editor(s). MDPI and/or the editor(s) disclaim responsibility for any injury to people or property resulting from any ideas, methods, instructions or products referred to in the content.